

31 mai 1996

5W9632

IPNO-DRE-96-11

CERN LIBRARIES, GENEVA



SCAN-9608010

*Characteristics of vaporization events :
is thermodynamical equilibrium achieved ?*

*B. Borderie, A. Chbihi, D. Durand, F. Gulminelli,
M. Parlog, M.F. Rivet, L. Tassan-Got et al*

Submitted to Physics Letters B

Characteristics of vaporization events: is thermodynamical equilibrium achieved?

B. Borderie¹, A. Chbihi², D. Durand³, F. Gulminelli³, M. Parlog^{1a}, M.F. Rivet¹, L. Tassan-Got¹,
G. Auger², Ch.O. Bacri¹, J. Benlliure², E. Bisquer⁴, R. Bougault³, R. Brou³,
J.L. Charvet⁵, J. Colin³, D. Cussol³, R. Dayras⁵, E. De Filippo⁵, A. Demeyer⁴,
D. Doré¹, P. Ecomard², P. Eudes⁶, D. Gourio⁶, D. Guinet⁴, R. Laforest³,
P. Lantesse⁴, J.L. Laville⁶, L. Lebreton⁴, J.F. Lecomte³, A. Le Fèvre²,
T. Lefort³, R. Legrain⁵, O. Lopez³, M. Louvel³, J. Łukasik^{1b}, N. Marie²,
V. Métivier^{3c}, L. Nalpas⁵, A. Ouatizerga¹, J. Péter³, E. Plagnol¹, A. Rahmani⁶,
T. Reposeur⁶, E. Rosato³, F. Saint-Laurent², M. Squalli¹, J.C. Steckmeyer³,
B. Tamain³, E. Vient³, C. Volant⁵, J.P. Wieleczko².

¹ *Institut de Physique Nucléaire, IN2P3-CNRS, 91406 Orsay Cedex, France*

² *GANIL, CEA, IN2P3-CNRS, B.P. 5027, 14021 Caen Cedex, France*

³ *LPC, IN2P3-CNRS, ISMRA et Université, 14050 Caen Cedex, France*

⁴ *IPN Lyon, IN2P3-CNRS et Université, 69622 Villeurbanne Cedex, France*

⁵ *CEA, DAPNIA/SPhN, CEN Saclay, 91191 Gif sur Yvette Cedex, France*

⁶ *SUBATECH, IN2P3-CNRS et Université, 44072 Nantes Cedex 03, France.*

Abstract

Properties of nearly all final products observed in particular heavy-ion collisions are presented. They concern the vaporization events detected with the 4π array INDRA, where all detected species have atomic numbers lower than 3. Data were obtained over a broad excitation energy range (8-28 A MeV). The occurrence of thermodynamical equilibrium is discussed by comparing the data with the results of two statistical models. Finally a comment is made on the temperature extracted from the $Z=1$ and $Z=2$ isotopic ratios in relation to findings obtained with heavier isotopes in another experiment.

The question of whether or not hot nuclear matter formed in violent heavy-ion collisions reaches thermodynamical equilibrium before starting to disassemble is of essential importance in validating the hypotheses assumed in statistical models^{1, 2, 3} and in constraining the ingredients entering microscopic models based on transport theories^{4, 5, 6, 7}. In particular, chemical equilibrium controls the yields of the different products and strongly influences the isotopic composition. Therefore, the experimental study of such an issue requires the detection and identification (mass and charge) of all or nearly all final products. This kind of measurement was recently achieved by studying with INDRA⁸ a particular class of events produced in $^{36}\text{Ar} + ^{58}\text{Ni}$ collisions, namely the vaporization events⁹. These events,

^apermanent address: *Institute of Physics and Nuclear Engineering, IFA, P.O. Box MG6, Bucharest, Romania*

^bpermanent address: *Institute of Nuclear Physics, ul. Radzikowskiego 152, 31-342 Kraków, Poland*

^cpresent address: *SUBATECH, IN2P3-CNRS et Université, 44072 Nantes Cedex 03, France*

where more than 90% of the charged particles were detected and isotopically identified, were properly characterized since the total number of - unmeasured - neutrons could be derived event by event from mass conservation. Vaporization events were observed and studied at 52,74,84 and 95 A MeV.

To correctly derive the properties of these events, the dynamics of the collisions must first be studied: are we dealing with the vaporization of one source, or of several sources? An answer to this question is given by the parallel velocity spectra of the particles (Fig 1): there is a clear asymmetry in the velocity spectrum of the α 's, and to a lesser extent in that of the protons, indicating the presence of two sources in most events.

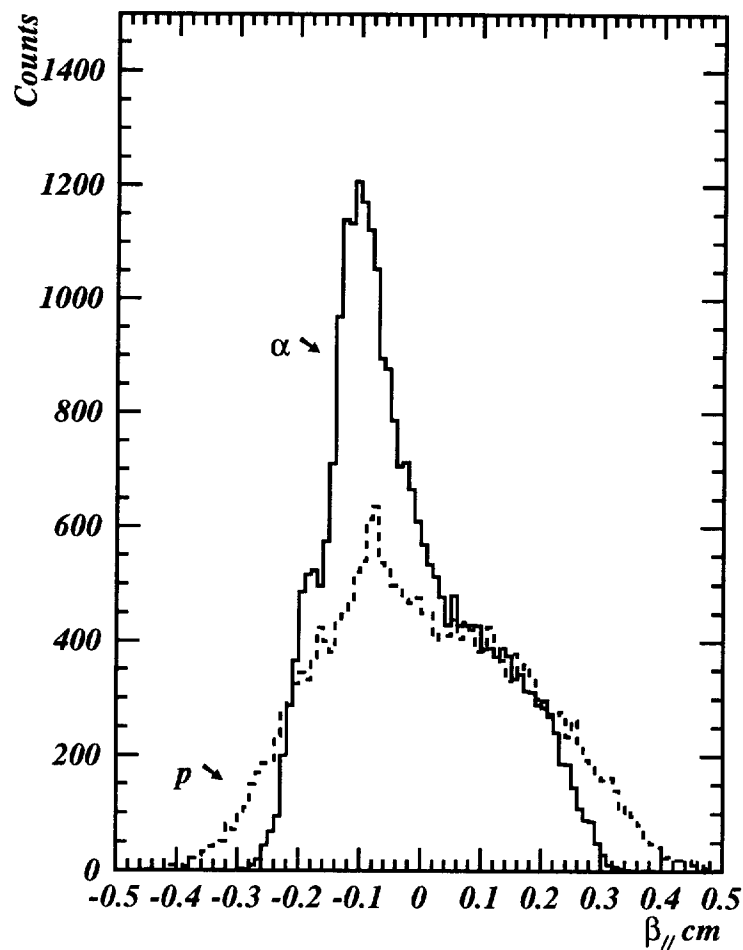


Figure 1: *Parallel velocity spectra, in the center of mass of the reaction, of protons and α particles for Ar+Ni collisions at 95 A MeV*

The use of global variables characterizing the shape of the events in momentum space leads to the same conclusion: only a small part of the events (around

10%, whatever the incident energy) could possibly be associated with the decay of a single source. These events are not included in the following analysis. Usually, for heavy systems, the source reconstruction make use of the heaviest products only. In a similar way, the subset of particles with masses larger than 2 was used here. These particles carry on average more than 50% of the total mass of the system. They should also be less sensitive to preequilibrium emission, if any is present, which should concern mostly nucleons. Owing to the large number of particles, we use a method similar to the "thrust" ¹⁰, but faster, to determine the source velocities. Then the dynamics of the reaction is fully fixed. A complete description of the determination of the dynamics of these collisions, and more specifically its influence on the variables described later on in this paper, will be presented in a forthcoming article ¹¹. The spectra of the relative velocity between the sources are broad, extending from 4. cm/ns up to 62,69,75,81 % of the beam velocity at 52,74, 84,95 AMeV respectively. This indicates:

- that the collisions leading to full vaporization of the system correspond to a broad range of impact parameters; this is in agreement with the transverse energy spectra of the vaporization events, from which the impact parameter range can be estimated between 0 and $0.4 b_{max}$.
- that for the bulk of the events the relative motion is far from being fully damped, and therefore a large fraction of the available energy remains as collective translational energy.

It is interesting to note that Landau-Vlasov simulations (implemented with the Gogny force ¹²) give results in agreement with the experimental findings ¹³, namely "binary" collisions for the whole impact parameter range, and relative velocities between the two final partners covering the experimental spectra for the same impact parameter range. Another point derived from these simulations is that, from 74 AMeV upwards, the emission flux of particles is found constant with time, contrary to what is observed at lower incident energy for which two regimes are clearly observed. This fact indicates that in this framework the distinction between preequilibrium and equilibrium emission becomes irrelevant.

To go further, one now needs the primary masses and excitation energies of the two sources. The measured particles not included in the reconstruction of the sources (p and d) are attributed to the source in which their relative velocity is smallest, without attempting to distinguish any preequilibrium emission. The energy spectra of each type of particle in each source frame are constructed, and it was checked that the forward and backward spectra in all situations were superimposable.

To perform full calorimetry, each event is then completed in charge according to the measured particle distribution, and all added charged particles are attributed to the slower source, assuming that the effects of the detection thresh-

olds overcome those of the geometrical efficiency. Neutron multiplicity then follows from mass conservation, and the neutrons are shared between the two sources by assuming that for each source $N \geq Z + 1$ (recalling that the total system has two extra neutrons with respect to isospin 0). The kinetic energies of the added particles are taken equal to the average energy of the same particle species in the events belonging to the same excitation energy bin; for neutrons one uses the average proton energy minus 2 MeV to take into account the Coulomb barrier. On average, the source masses are found close (38 and 56 at all energies) to the initial projectile and target masses, but with large fluctuations. In the following the sources will then be called quasi-projectile (QP) and quasi-target (QT). The excitation energy of each source is calculated as

$$E_S^* = \sum_i (\Delta m_i + E_{K_i}) - \Delta m_S, \quad (1)$$

Δm_i being the mass excess of particle i , Δm_S that of the source, and E_{K_i} the i th particle kinetic energy in its source frame. As expected from the relative velocities broad spectra, the excitation energy spectra of each source are also very broad. Whatever the incident energy and the source (QP or QT) the excitation energy distributions start rising around 8 AMeV, while the maximum excitation energy reached increases with the incident energy, up to 28 AMeV (for the QP) at 95 AMeV. The mean values and the standard deviations of the excitation energy distributions are listed in table 1.

E_{beam} AMeV	52	74	84	95
E_{avail} MeV	1162	1594	1861	2075
$\langle E^* \rangle$ QP MeV	393±112	535±168	594±195	666±216
$\langle E^* \rangle$ QT MeV	483±110	683±169	744±186	822±203
$\langle E_{trans} \rangle$ MeV	258±81	409±118	472±147	563±183
$\langle \epsilon^* \rangle$ QP AMeV	10.1±2.5	14.3±3.2	15.7±3.6	17.7±3.9
$\langle \epsilon^* \rangle$ QT AMeV	8.8±1.8	12.0±2.4	13.2±2.7	14.6±3.0

Table 1: Available energy, mean values \pm standard deviations of the excitation energy distributions of the QP and QT, of the translational kinetic energy distribution, and of the excitation energy per nucleon distributions of the QP and QT, versus the incident energy.

In all cases the heavy source (QT) has more excitation energy than the light one (QP), but the QP has a higher excitation energy *per nucleon* than the QT, which means that thermal equilibrium is not achieved between the two partners of the collision, due to the very short reaction time (≤ 100 fm/c¹³). The energy equilibration time was estimated to be 150-300 fm/c in ref¹⁴. Whether or not each sub-ensemble subsequently reaches thermal or thermodynamical (thermal and chemical) equilibrium before disintegrating can be investigated by looking at the particle energy spectra and relative abundances in each source,

as a function of its excitation energy per nucleon, ϵ^* ; a binning $\delta\epsilon^*=3\text{MeV}$ was chosen.

We discuss first the shapes of the kinetic energy spectra which give information about thermal equilibrium for each source. Some examples of spectra are displayed (Fig 2-a) which concern particles emitted by the QP with an average excitation energy of $18.5 \text{ AMeV} \pm 1.5 \text{ AMeV}$ corresponding to the most probable value (see inner picture in Fig 2-b). They are structureless, with exponential tails whose slopes are similar within 30%. More quantitatively, for the emission from a source in thermal equilibrium, all particles should have the same average kinetic energy if we neglect in a first approximation the possible Coulomb barrier. An example of the evolution of the average kinetic energy of each particle species is given in fig 2-b, for the QP at 95 AMeV. The increase of the kinetic energy with the excitation energy is almost linear for all particles; there is a gap between the more energetic particles (d and ^3He) and the less energetic ones (p and ^4He) of 4-7 MeV or $\sim 20\%$. This may appear as a significant deviation from thermal equilibrium. If we note that no extra collective expansion energy (proportional to the atomic mass) can be derived from the data, the eventual role of quantal effects and side-feeding has to be checked. In order to test this hypothesis we have modelled the emitting sources using two different approaches based on thermodynamical equilibrium. In the first model, hereafter denoted EVA, we use the Weisskopf standard evaporation theory ¹⁵, by considering a series of binary break-ups into excited fragments ¹⁶. The level density parameter is taken equal to $A/10$. The discrete levels of light nuclei (up to ^9B) are taken into account, as well as Coulomb effects in the exit channels. This approach is expected to be valid only at rather low excitation energies. In the second model (CEM), which is expected to be more suited to describe the situation discussed here, the emitting source is viewed as a nuclear gas in thermal and also chemical equilibrium ¹⁷. In this simple model for a given source density ρ and temperature T , the energy spectra of the different nuclear species (and consequently their relative yields) are uniquely determined from conservation laws and the equilibrium distributions in the grandcanonical ensemble

$$n_i(e) = f_Q(e, \mu_i, T) \quad i = 1, \dots, N \quad (2)$$

where N is the number of species taken into account (limited here to nuclear states which deexcite in $Z=0,1,2$, up to ^9B), f_Q is the density of occupied states taking into account the appropriate quantum statistics (Fermi or Bose) and μ_i is the chemical potential of the species i , which is a function of the break up density ρ via the neutron and proton chemical potentials μ_N, μ_Z

$$\mu_i = \mu_N N_i + \mu_Z Z_i + B_i \quad (3)$$

Here, N_i, Z_i are the neutron and proton number of the isotope under consideration and B_i its binding energy. All excited states with a width smaller than

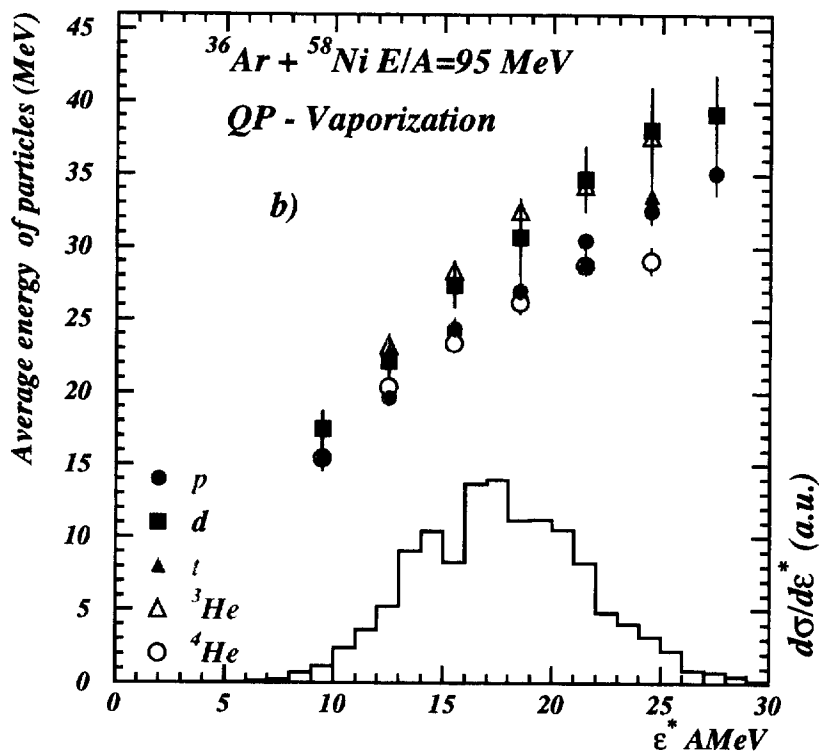
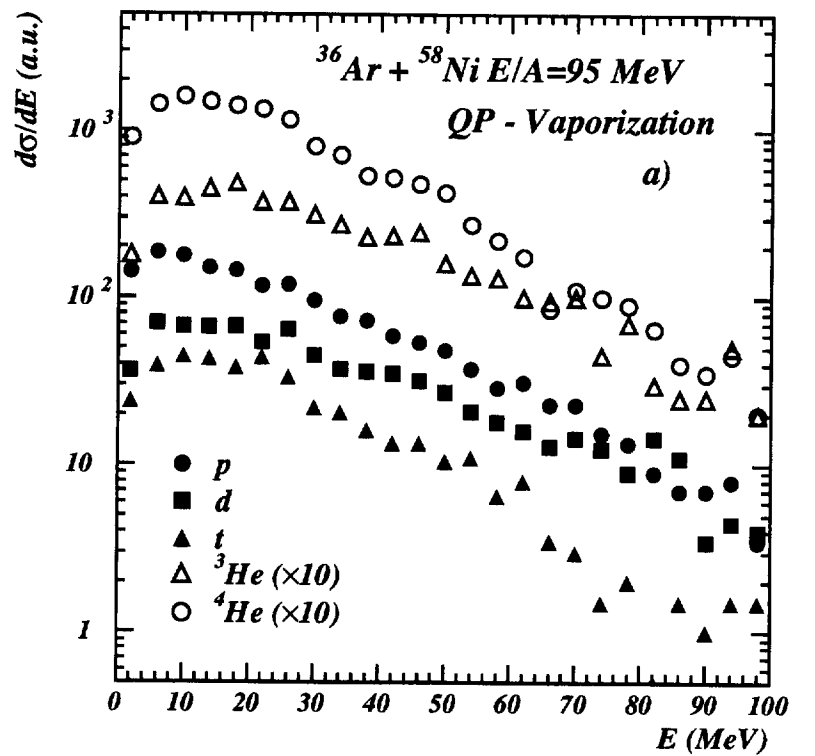


Fig 2: a) Kinetic energy spectra of the different species emitted in vaporization of the QP for an average excitation energy of 18.5 A MeV. The spectra are calculated in the center-of-mass of the QP. b) Average kinetic energies of the different particles attributed to the QP as a function of the QP excitation energy. The histogram represents the excitation energy distribution.

1 MeV are taken into account, and the final distributions are corrected for the side-feeding of resonance decay¹⁶. Corrections to the ideal gas are also included in the form of excluded volume effects¹⁸. In this calculation ϵ^* is derived, as in the experiment, from calorimetry. The experimental ϵ^* range is covered by varying T from 10 to 25 MeV. The freeze out density has been fixed to $\rho = \rho_0/3$, in order to reproduce the experimental ratio between the proton and alpha yields at the lowest excitation energy. The results are however not very sensitive to this parameter, in a reasonable range of freeze out densities from $\rho = \rho_0/2$ to $\rho = \rho_0/5$. Some results of these two models are compared to the data in table 2. In EVA the calculation was performed taking A=36 and Z=18 as QP.

Particle	$\langle E \rangle_{exp} (MeV)$	$\langle E \rangle_{EVA} (MeV)$	$\langle E \rangle_{CEM} (MeV)$
n		19.6.	28.0
p	27.0 ± 0.4	23.4.	31.1
d	30.7 ± 0.6	23.7.	27.0
t	27.3 ± 0.8	22.7.	29.3
³ He	32.6 ± 0.9	23.1.	29.6
α	26.2 ± 0.3	20.6.	32.5

Table 2: Comparison between experimental average kinetic energies and the results of the two models described in the text, for vaporization of the QP at $\epsilon^* = 18.5$ MeV.

EVA gives kinetic energies which are systematically too low whereas CEM reproduces rather well the measured values. Both models fail to accurately follow the dependence on the different species. The energy differences between particles in the CEM model are due to the different statistics (Fermi or Bose) and to side-feeding. This last effect may be partially biased by the limited number of species included in the model. Another limitation, which holds for both models, comes from the incomplete knowledge of the branching ratios of the different decay channels for particle-unstable resonances. Finally, the quality of agreement of the two models with the data remains approximately the same over the whole excitation energy range.

We now come to the chemical composition of the vaporized source. In Fig 3-a,-b is shown the relative particle abundance ($P_j = M_j/M_S$, where M_S is the total source multiplicity and M_j the multiplicity of particle species j in the source) versus the source excitation energy, for the QP at 95 A MeV. α -particles dominate at the lower excitation energies, while nucleons take over when the excitation energy is increased. The deuteron relative abundance is roughly constant; the isobars of mass 3 have opposite behaviours: tritons decrease and ³He increase when raising the energy. Finally the rare ⁶He behave like the α 's. This evolution is not due to autocorrelations between the source composition and its excitation energy. Indeed, the mass excess part in eq. 1 accounts for

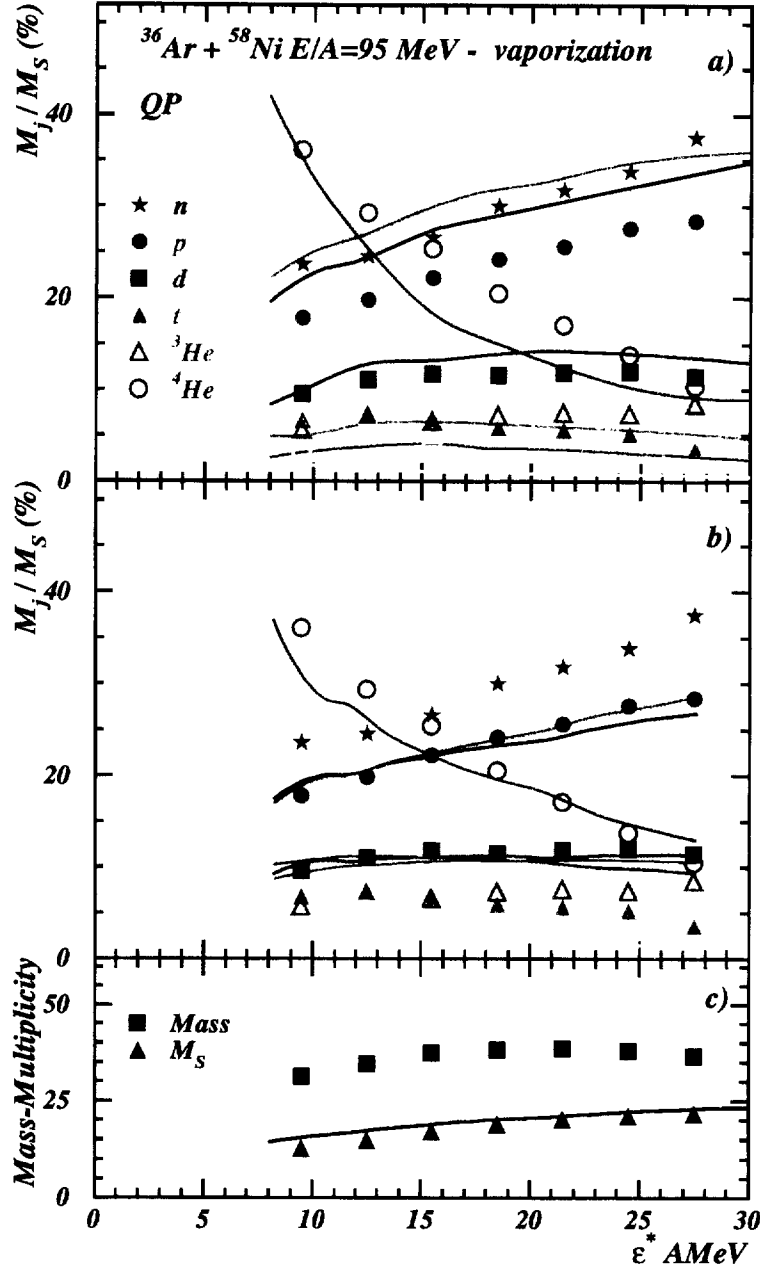


Fig 3: a) Composition of the QP as a function of its excitation energy. Symbols are for data while the different lines with corresponding colors are the results of the model (EVA) discussed in the text. b) Same as before but the lines are here the results of the model (CEM) discussed in the text. c) Experimental average mass and total multiplicity of the QP. The line is the result for multiplicity of the model (EVA) with a constant mass $A=36$.

~ 40% of the excitation energy around 10 AMeV, and only 20% around 22 AMeV. Therefore the increase of the source excitation energy is not only due to the increase of the nucleon abundance, but also to the increase of the kinetic energy of the particles. Note that for a given ϵ^* the relative yields are the same for the QP and the QT, independently of the bombarding energy. For a system without isospin like the one under consideration here, equal abundances of t and ${}^3\text{He}$, and of p and n, are expected from chemical equilibrium, while they show slight differences in our data. Once again the significance of these differences has to be tested against models. EVA and CEM reproduce well the general evolution of the different species as a function of the excitation energy. In EVA the lack of kinetic energies (table 2) has to be compensated by nucleon creation in order to conserve the energy; indeed the yield of protons is strongly overestimated while the production of Z=2 species is too low (fig. 3a). Otherwise the hierarchy of particle yields is roughly reproduced as well as the total multiplicity (fig. 3c). Concerning the prompt scenario, for which the ratio between the proton and alpha yields was fixed at the lowest excitation energy, the yields of these two species are correctly reproduced as well as those of deuterons and ${}^6\text{He}$. The production of isobars of mass 3 is overestimated by a factor of two (fig.3b). To further understand the significance of the observed deviations with CEM, it would be interesting to also compare the data with a more sophisticated model like the QSM of ref ³, where the contribution from higher-lying resonances is taken into account.

Recently a method for obtaining nuclear temperatures with the help of the yields of different species (double ratios of two isotope pairs) ¹⁹ was used by the authors of ref. ²⁰ to study the caloric curve, i.e the correlation between the excitation energy and the temperature. If one assumes that the system is in thermodynamical equilibrium, and at low density, when using isotopes of Z=1 and 2, the temperature is written as:

$$T = 14.3 \cdot \text{Log}^{-1} \left(1.6 \frac{Y(d)Y(\alpha)}{Y(t)Y({}^3\text{He})} \right) \quad (4)$$

where the Y's are the measured yields. This "temperature" can be calculated as a function of the excitation energy and exhibits a linear increase of T with ϵ^* , from $T \sim 5.2$ MeV at $\epsilon^* \sim 8 \text{ AMeV}$ to $T \sim 7.5$ MeV at $\epsilon^* \sim 25 \text{ AMeV}$. The sudden change of slope around $\epsilon^* = 10$ AMeV, observed in ref ²⁰ from different isotope pairs, is not present in our data. Similar studies for other classes of events (those containing fragments), using the same isotopes, are under way and give the same "temperature" values ²¹.

In conclusion, vaporization events have been studied in a broad excitation energy range from 8 to 28 AMeV. They are produced in binary collisions. After reconstruction of the two sources of emission, the yields and the energy spectra of the different species have been studied and compared with the predictions of

two statistical models. The model describing the properties of a gas of fermions and bosons in thermal and chemical equilibrium reproduces rather well both the energies and the yields suggesting that thermodynamical equilibrium may have been reached by each source.

We are grateful to Ph. Chomaz for interesting discussions and help in the development of the CEM model.

References

1. J. Bondorf et al, *Nucl. Phys.* **A443** (1985) 321, **A444** (1985) 460, **A448** (1986) 753.
2. D.H.E. Gross, *Rep. Prog. Phys.* **53** (1990) 605. and references therein
3. H. Stoecker and W. Greiner, *Phys. Rep.* **5** (1986) 277
J. Konopka et al, *Phy. Rev.* **C50** (1994) 2085.
4. G. Bertsch and S. Das Gupta, *Phys. Rep.* **160** (1988) 189
5. J. Aichelin, *Phys. Rep.* **202** (1991) 233
6. A. Bonasera, F. Gulminelli, J. Molitoris, *Phys. Rep.* **243** (1994) 1
7. D. Idier et al, *Ann. Phys. Fr.* **19** (1994) 159
8. J. Pouthas et al, *Nucl. Instr. Meth. in Phys. Res.* **A357** (1995) 418, **A369** (1996) 222.
9. C.O. Bacri et al, *Phys. Lett.* **B353** (1995) 27.
10. J. Cugnon and D. L'Hote, *Nucl. Phys.* **A397** (1983) 519.
11. INDRA collaboration, to be published.
12. J. Dechargé and D. Gogny, *Phys. Rev.* **C21** (1980) 1568.
13. P. Eudes et al, in preparation.
14. B. Borderie et al., *Z. Phys A - Hadrons and Nuclei* **338** (1991) 369.
15. V.F. Weisskopf, *Phys. Rev.* **52** (1937) 295
16. D. Durand et al, code SIMON in preparation
17. A.Z. Mekjan, *Phys. Rev. C* **17** (1978) 1051
18. R. K. Tripathi and L.W. Townsend, *Phys. Rev. C* **50** (1994) R7
19. S. Albero et al, *Nuovo Cimento* **A89** (1985) 1.
20. J. Pochodzalla et al, *Phys. Rev. Lett.* **75** (1995) 1040.
21. INDRA collaboration, to be published.